First passage time distribution of chaperone driven polymer translocation through a nanopore: Homopolymer and heteropolymer cases

Rouhollah Haji Abdolvahab, Ralf Metzler, and Mohammad Reza Ejtehadi

Citation: J. Chem. Phys. **135**, 245102 (2011); doi: 10.1063/1.3669427
View online: http://dx.doi.org/10.1063/1.3669427
View Table of Contents: http://jcp.aip.org/resource/1/JCPSA6/v135/i24
Published by the American Institute of Physics.

First passage time distribution of chaperone driven polymer translocation through a nanopore: Homopolymer and heteropolymer cases

Rouhollah Haji Abdolvahab,[1,a)] Ralf Metzler,[2,3] and Mohammad Reza Ejtehadi[1]
[1]*Physics Department, Sharif University of Technology, P.O. Box 11155-9161, Tehran, Iran*
[2]*Institute for Physics and Astronomy, University of Potsdam, 14476 Potsdam-Golm, Germany*
[3]*Department of Physics, Tampere University of Technology, FI-33101 Tampere, Finland*

(Received 8 June 2011; accepted 21 November 2011; published online 23 December 2011)

Combining the advection-diffusion equation approach with Monte Carlo simulations we study chaperone driven polymer translocation of a stiff polymer through a nanopore. We demonstrate that the probability density function of first passage times across the pore depends solely on the Péclet number, a dimensionless parameter comparing drift strength and diffusivity. Moreover it is shown that the characteristic exponent in the power-law dependence of the translocation time on the chain length, a function of the chaperone-polymer binding energy, the chaperone concentration, and the chain length, is also effectively determined by the Péclet number. We investigate the effect of the chaperone size on the translocation process. In particular, for large chaperone size, the translocation progress and the mean waiting time as function of the reaction coordinate exhibit pronounced sawtooth-shapes. The effects of a heterogeneous polymer sequence on the translocation dynamics is studied in terms of the translocation velocity, the probability distribution for the translocation progress, and the monomer waiting times. © *2011 American Institute of Physics*. [doi:10.1063/1.3669427]

I. INTRODUCTION

Translocation, the passage of biopolymers such as proteins, DNA, and RNA through narrow channels in lipid membranes is a quite ubiquitous process of fundamental importance in biology and biotechnology. Such channels in biological cells are constituted by specific channel proteins, such as the ones of the haemolysin family. Particularly common is the channel protein α-haemolysin, that is also employed in numerous setups *in vitro*. Alternatively, silicon based compound solid state nanopores are used. The significance of translocation thereby encompasses pure transport of polymers through the channel, but also applications to chain sequencing and drug delivery.[1–4] Due to an entropic barrier thwarting the passage of the polymer as a result of constrictions imposed by the pore confinement, efficient polymer translocation requires a driving force. Such a force could be purely entropic itself, for instance, it could emerge from spatial confinement of the chain-to-be-translocated in a virus capsid, a membrane vesicle, or confinement in nanofluidic setups.[5–7] Alternatively, both in living cells and *in vitro*, charged chains may be driven by cross-membrane electrical potential differences, a method that has so far received most experimental and theoretical attention.[5,8–16] While usually the length of the pore is considered much less than the length of the translocating polymer, in modern nanofluidic setups long nano-sized channels are used, whose length is much larger than the chain's.[17] In such cases, the driving force is proportional to the length of the chain inside the channel.[18]

Here we consider yet another driving mechanism, which is quite widespread in nature. Namely, we consider the effective chemical potential difference between cis and trans side of the pore, effected by binding proteins called chaperonins or chaperones.[1,19–33] Chaperone-driving is particularly common in eukaryotic mitochondria.[1] Chaperones exist in different concentrations on the cis and trans sides. Once (reversibly) bound to the chain, they prevent back-sliding of the chain through the pore, and thus partially ratchet the translocation, as sketched in Fig. 1. To pinpoint the effects of the chaperone-driving mechanism, in agreement with the majority of previous studies we consider a chain with large persistence length compared to the chain length (stiff chain limit), such that we can neglect polymeric degrees of freedom, which strongly change the dynamics of the translocation process. The length of the chain-to-be-translocated in our study is $L = M\sigma$, where M is the number of monomers of individual size σ. We also assume that chaperones are only present on the trans side of the pore. The size of the chaperones is $\lambda\sigma$, where λ is typically larger than 1. In our previous work we combined a Monte Carlo simulation approach with a mean field theory,[22] showing that by variation of the effective binding energy (EBE),

$$\mathcal{E}^i_{\rm eff} = -\frac{1}{\lambda}\log\left[c_0 v_0 \exp\left(-\frac{\varepsilon_i}{k_B T}\right)\right], \qquad (1)$$

the translocation dynamics changes continuously from purely diffusive to ballistic translocation. In Eq. (1), ε_i is the chaperone binding energy per monomer of the polymer, c_0 the chaperone concentration, and v_0 their eigenvolume. The term $c_0 v_0$ is thus the probability that a chaperone is next to a given binding site.[22] In Ref. 22 we also considered effects of the sequence of sites with different binding affinity to the chaperones on the translocation time.

a)Author to whom correspondence should be addressed. Electronic mail: abdolvahab@physics.sharif.edu.

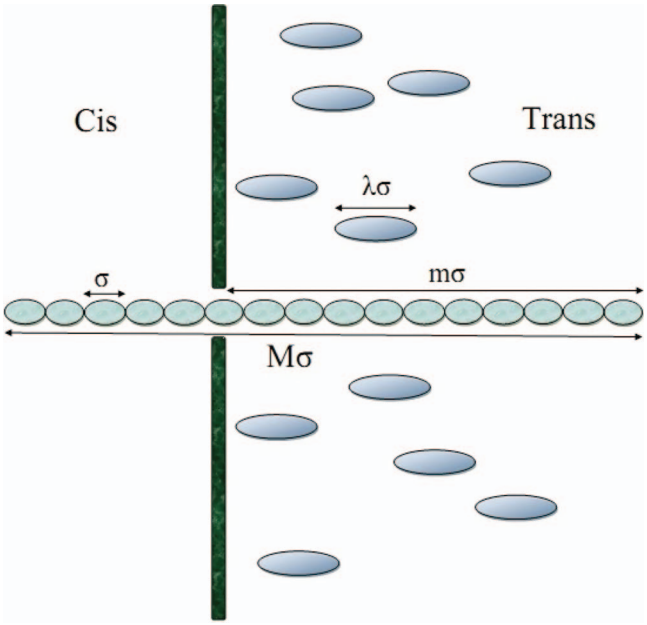

FIG. 1. Translocating polymer consisting of monomers of size σ. On the trans side binding proteins (chaperones) of size $\lambda\sigma$ bind to the translocating chain, giving rise to a chemical potential difference. The number m of already translocated monomers is a natural "reaction coordinate" of the translocation process.

Here, we study in a continuous advection-diffusion model the probability density function (PDF) for translocation times as a first passage problem.[34] The model predictions are compared with results from Monte Carlo simulations. Interestingly, we find that the PDF of translocation times is solely determined by the dimensionless Péclet number

$$\mathrm{Pe} = \frac{LV}{2D}, \tag{2}$$

where V is the mean translocation velocity and D the diffusivity of the chain. The Péclet number, technically equivalent to the product of the Reynolds and Prandtl numbers, compares the strength of advection to the thermal diffusivity. It vanishes for unbiased diffusion. The Péclet number will be shown to determine the characteristic exponent of the translocation time as function of the chain length. In the following, we also study the effect of the chaperone size λ and of a heterogeneous sequence of chain monomers with different chaperone affinity on the process, finding a pronounced sawtooth-pattern for the probability distribution of the translocation progress and the mean waiting time as function of the reaction coordinate m (Fig. 1).

In what follows, we first introduce our theoretical model. Its results are compared to simulations results in Sec. III, followed by a discussion of the effects of the chaperone size on the translocation pattern in Sec. IV. We draw our conclusions in Sec. V.

II. DRIFT-DIFFUSION MODEL

Theoretically, the polymer translocation can be described by a bivariate master equation of the form

$$\frac{\partial}{\partial t} P^*(m,n,t) = \mathbb{L}^*(m,n) P^*(m,n,t), \tag{3}$$

where $P^*(m, n, t)$ is the probability distribution to find the translocating chain at reaction coordinate m (m monomers have passed the pore), and with n chaperones bound to it on the trans side, at time t. The operator $\mathbb{L}^*(m, n)$ then details the incoming and outcoming fluxes from state (m, n), i.e., backward/forward motion of the chain through the channel and chaperone binding/unbinding.[22,29,30,32] Under the assumption that the dynamics of chaperone (un)binding is fast compared to the diffusive motion of the chain by one monomer's distance, we adiabatically eliminate the number n of bound chaperones from Eq. (3). Given that the chain's longitudinal diffusivity in free space is inversely proportional to the number M of monomers and even slower when passing through the pore channel,[35] for sufficiently long chains and high chaperone concentrations the assumption of comparatively fast chaperone (un)binding dynamics is reasonable. The procedure of adiabatic elimination of n from Eq. (3) yields the master equation

$$\begin{aligned}\frac{\partial P(m,t)}{\partial t} &= \mathbb{L}(m)P(m,t)\\ &= W^+(m-1)P(m-1,t)\\ &\quad + W^-(m+1)P(m+1,t)\\ &\quad - [W^+(m)+W^-(m)]P(m,t),\end{aligned} \tag{4}$$

where $W^+(m)$ and $W^-(m)$ are, respectively, the transition rates for forward and backward motion, further specified below. Thus, the first term on the right hand side of Eq. (4) denotes an increase of the reaction coordinate by 1 from $m - 1$ to m, i.e., the chain-to-be-translocated moves to the trans side, while the second term corresponds to stepping back to the cis side by one monomer, etc. $P(m, t)$ is the probability distribution of finding m monomers of the chain to the right of the pore at time t. The slowness of the diffusive steps of the translocation process also ensures that we may assume detailed balance to hold for the forward and backward rates in the associated operator $\mathbb{L}(m)$, compare the discussion in Ref. 30.

Let us now specify the rates W appearing in Eq. (4). To this end, we note that in our model we do not have any chaperones on the cis side of the membrane. Thus, feeding of the chain to the trans side by one monomer step ($m \to m + 1$) corresponds to the constant rate $W^+(m) = k \equiv 1/2\tau_0$, where τ_0 is the typical time it takes the bare chain to diffuse over the distance σ of the monomeric size, i.e., $\tau_0 \approx \sigma^2/(2D)$. The factor $1/2$ in the expression for W^+ is introduced due to the fact that only half of all diffusion attempts go in the direction of the trans side. By virtue of the detailed balance condition the backward rate $W^-(m)$ then follows in the form $W^-(m) = k\mathscr{Z}(m-1)/\mathscr{Z}(m)$,[29,30,32] where $\mathscr{Z}(m)$ is the partition function of the translocation problem. In a mean field sense, we introduce the effective chaperone binding probability P per monomer of the chain-to-be-translocated. Physically, the backsliding of the chain through the pore can only occur when no chaperone is bound to the chain at the monomer immediately to the right of the pore. The associated probability is $1 - P$, so that the backward rate becomes $W^-(m) = 1/(2\tau_0)(1 - P)$. P depends on the

binding energy between a chaperone and the chain monomers it covers, as well as the chaperone concentration.[22] However, while the choice of the constant k for the rate W^+ directly mimics the physical picture of the forward motion, we note that we have a freedom of choice for the rates W^+ and W^-.[36] For the sake of retrieving a true diffusion *constant* in the desired continuum limit, we prefer the following choice for the forward and backward rates:

$$W^+(m) = \frac{1}{2\tau_0}\left(1 + \frac{P}{2}\right), \tag{5}$$

$$W^-(m) = \frac{1}{2\tau_0}\left(1 - \frac{P}{2}\right). \tag{6}$$

With above rates (5) and (6) the average velocity of the polymer becomes[36]

$$V = \sigma(W^+ - W^-) = \frac{\sigma}{2\tau_0}P, \tag{7}$$

while we obtain

$$D = \sigma^2\left(\frac{W^+ + W^-}{2}\right) = \frac{\sigma^2}{2\tau_0} \tag{8}$$

for the diffusion coefficient. Thus, the drift velocity (7) is linear in the binding probability and vanishes in the absence of chaperones. The diffusion coefficient (8) according to our choice of the transfer rates (5) and (6) is independent of the binding probability. With the quantities (7) and (8) we obtain the diffusion advection equation for chaperone driven polymer translocation in the form

$$\frac{\partial \mathcal{P}(x,t)}{\partial t} + V\frac{\partial \mathcal{P}(x,t)}{\partial x} = D\frac{\partial^2 \mathcal{P}(x,t)}{\partial x^2}, \tag{9}$$

as the continuum limit of the master equation (4) in the mean field sense. In Eq. (9), we define the continuous coordinate $x = m\sigma$. The quantity $\mathcal{P}(x,t)$ denotes the probability density to find the chain at translocation coordinate x at time t (see Appendix A). The initial condition is to start from $x = 0$, $\mathcal{P}(x,0) = \delta(x)$. The boundary conditions are reflective on the left at $x = 0$, corresponding to the assumption that the chain is not allowed to fully retract from the pore. On the right at $x = L = M\sigma$, we impose an absorbing boundary condition, mirroring our goal to determine the first passage time for the translocation process. In this so-called transmission mode, the dynamic equation (9) allows for an explicit solution in Laplace space.[34] As a result, the Laplace transform

$$j(L,s) = \int_0^\infty j(x,t)e^{-st}dt\Big|_{x=L}. \tag{10}$$

of the probability flux at the right can be written as

$$j(L,s) = \frac{P_s e^{\mathrm{Pe}}}{\mathrm{Pe}\sinh(P_s) + P_s\cosh(P_s)}, \tag{11}$$

where

$$\mathrm{Pe} = \frac{VL}{2D} = \frac{1}{2}PM \tag{12}$$

is the Péclet number; a dimensionless parameter comparing the respective intensity of drift and diffusion.[34] At large Péclet numbers, we are in a drift-dominated regime, while at small values of Pe, thermal fluctuations driving the diffusion are dominant. Moreover, in Eq. (11) we introduced the dimensionless quantity

$$P_s = L\sqrt{\frac{V^2}{4D^2} + \frac{s}{D}} = M\sqrt{\frac{P^2}{4} + 2\tau_0 s}. \tag{13}$$

The Laplace inverse of the flux, $j(L,t)$ corresponds to the probability density function (PDF) of first passage for complete translocation. Its corresponding moments can be obtained by Taylor expansion, following the procedure outlined in Ref. 34. In particular, for the mean first passage time we find

$$T = \frac{L^2}{D}\left[\frac{1}{2\mathrm{Pe}} - \frac{1}{4\mathrm{Pe}^2}(1 - e^{-2\mathrm{Pe}})\right]. \tag{14}$$

Differentiation of $\ln(T)$ with respect to L yields the scaling exponent α of the relation $T \sim L^\alpha$ in the form

$$\alpha = L\frac{\partial}{\partial L}\ln(T) = 1 + \frac{1 - (1 + 2\mathrm{Pe})e^{-2\mathrm{Pe}}}{2\mathrm{Pe} - 1 + e^{-2\mathrm{Pe}}} \tag{15}$$

For small values of the Péclet number, the asymptotic behavior becomes

$$\alpha \approx 2 - \frac{2}{3}\mathrm{Pe} + \frac{2}{9}\mathrm{Pe}^2, \tag{16}$$

while in the limit of large values of *Pe*, the dominating term is

$$\alpha \approx 1 + \frac{1}{2\mathrm{Pe}}. \tag{17}$$

Thus, as expected, the value of the scaling exponent α continuously changes from 2 for small Péclet numbers to 1 for large Pe, that is, from purely diffusive behavior to fully ballistic translocation. The binding probability as mean field parameter can be obtained from the relation

$$P = \frac{\exp\left(\Sigma_{i=1}^{\lambda}\mathcal{E}_{\mathrm{eff}}^i\right)}{1 + \exp\left(\Sigma_{i=1}^{\lambda}\mathcal{E}_{\mathrm{eff}}^i\right)} \tag{18}$$

in which $\mathcal{E}_{\mathrm{eff}}^i$ is the effective binding energy between monomer i and a chaperone, defined in Eq. (1). Thus, for a homopolymer the Péclet number simplifies to

$$\mathrm{Pe} = \frac{M}{2}\frac{\exp(\lambda\mathcal{E}_{\mathrm{eff}})}{1 + \exp(\lambda\mathcal{E}_{\mathrm{eff}})}, \tag{19}$$

where λ is the length of BPs.

Fig. 2 shows the variation of the scaling exponent α versus the Péclet number from Eq. (15), from diffusive to ballistic motion. The inset depicts the dependence of α on the EBE for 3 different chain lengths, demonstrating the non-universality of α with respect to the chain length.

III. COMPARISON WITH SIMULATIONS

In this section, we compare above results from the simple drift-diffusion model with simulations of chaperone-driven translocation of a stiff polymer chain. Similar to the quality of an analogous drift-dominated approach for driven translocation reported in Ref. 16, our model for chaperone driving is observed to be in excellent agreement with detailed simulations (compare Appendix C).

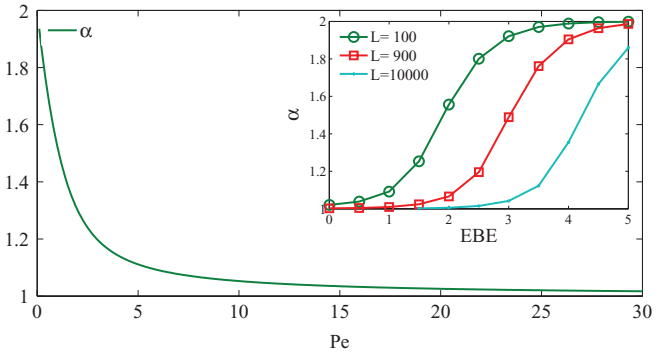

FIG. 2. It shows scaling exponent α ($T \sim M^{\alpha}$), from Eq. (15) versus Péclet number. The inset also shows α versus EBE for 3 different lengths.

A. Homopolymer chain

We start with the discussion of the behavior of the PDF of first passage of the chain across the pore as well as the scaling exponent α defined in Eq. (15), for the case of a homopolymer chain, i.e., all chain monomers are identical. In Subsection III B we turn to the case of a heteropolymer chain.

Fig. 3 compares the theoretical first passage PDF, calculated from Eq. (11), with simulations performed over 10^5 time steps (see Appendix C). We observe excellent agreement over the whole range of the PDF for chain length $M = 100$ and chaperone size of $\lambda = 2$ monomer lengths, for positive values of the EBE. Results for negative EBEs are good for the mean first passage time, however, the agreement with the overall PDF is less satisfactory (results not shown here). The reason is that for negative EBE the binding dynamics is dominated by few events, and thus the justification for the adiabatic elimination of the (un)binding dynamics of the chaperones is no longer given. In this case, Fig. 3 corroborates the usefulness of the continuum approach in terms of Eq. (9).

In Fig. 4 we plot the scaled PDF of translocation times for different values of the Péclet number. It shows how the PDF changes from a broad distribution in the diffusion dominated regime at small Pe to a significantly narrower distribution in the regime of drift domination (large

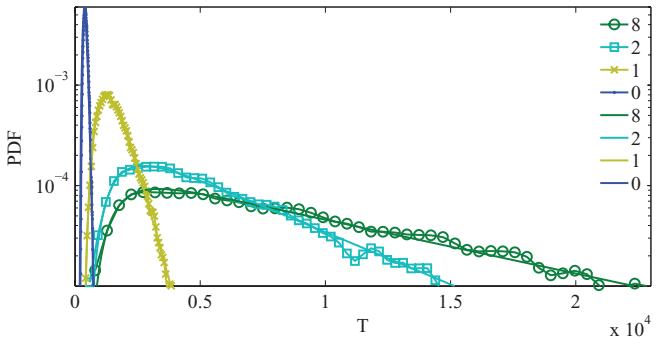

FIG. 3. Compare the probability density function(PDF) of translocation time that is obtained from simulation by theory. The markers show simulation results and the lines represent theory (Eq. (11)). The theory and simulation are in good agreement with each other in special for positive EBE. Numbers in the figure legends shows the EBE in k_BT.

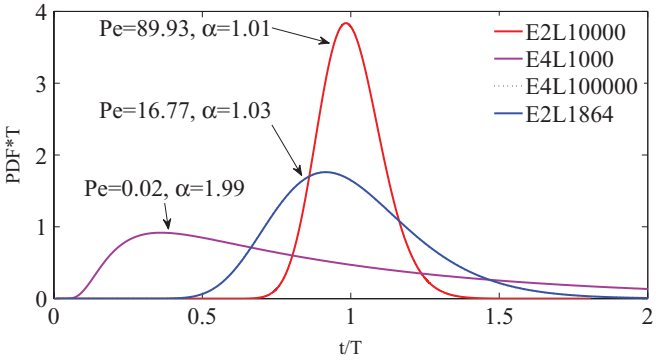

FIG. 4. Compare the probability density function(PDF) of translocation time for different length and different EBE that has been obtained from theory (Eq. (11)). The numbers in the legends are EBE (in k_BT) and length; for example E2L10000 means that the $EBE = 2$ and $M = 10000$. In middle, we plot PDF of translocation time for two polymers with different length and EBE, but the same Pe that as can be seen are exactly the same.

Pe). As demonstrated in the intermediate case, distributions for two polymers with different length and different EBE but the same Pe show indistinguishable forms of the PDF.

One of the most important parameters in polymer translocation is the scaling exponent α in the mean first passage time versus chain length dependence, $T \simeq M^{\alpha}$. To determine the exponent α reliably from simulations is a very time consuming process, as it requires the repeated performance of translocation of sufficiently long chains, in order to observe a sufficiently significant scaling window. As we showed recently,[22] the scaling exponent α in this problem depends on length, binding energy, and concentration of binding proteins; based on a simple mean field theory, we discussed that the Péclet number is the characterizing parameter for this problem. Here we demonstrate that the first passage time PDF obtained from our continuous model for various parameters agrees nicely with the simulations over the entire range. It turns out that the only relevant parameter is the Péclet number, as demonstrated in Fig. 4. Thus, chaperone driven polymer translocation of a stiff homopolymer is, to a good approximation, completely defined by the value of the Péclet number Pe. The scaling exponent α then follows from Eq. (15).

From Eq. (14) we obtain the reciprocal velocity $1/\langle V\rangle$[37] as function of the binding probability P, in the form

$$\frac{1}{\langle V\rangle} = \frac{\sigma}{DP}\left[1 - \frac{1}{MP}(1 - e^{-MP})\right]. \tag{20}$$

It varies from $\sigma/(DP)$ at $PL \gg 1$ to a plateau of value $L/(2D)$ at $PL \ll 1$. Fig. 5 depicts this behavior for a chain of length $M = 100$ and varying EBEs, i.e., different binding probabilities. The comparison with the simulations results shows good agreement at smaller values of P^{-1}, while a lesser deviation is observed at larger values of P^{-1}. This is most likely due to finite size effects, i.e., small numbers of bound chaperones.

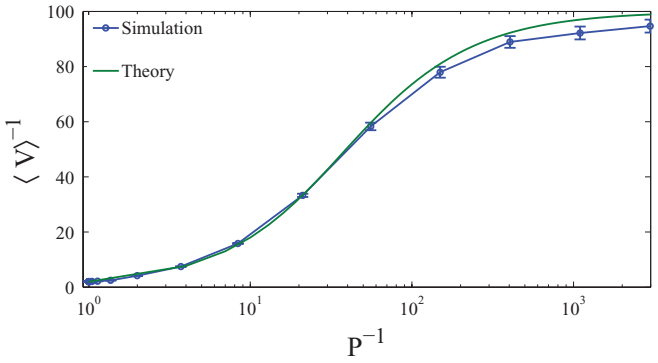

FIG. 5. Plot the inverse velocity of polymer that is obtained from simulation by theory (Eq. (20)) with respect to inverse binding probability (inset is the same but with zoom on small numbers).

B. Heteropolymer chain

Let us now address the translocation dynamics for the case of a heteropolymer chain, i.e., a chain consisting of monomers with different identity. A chaperone is assumed to feature different binding affinities to each of the monomer types. For simplicity we consider the minimal case of two monomer species, say, A and B. We also restrict our discussion to binding proteins, that cover $\lambda = 2$ chain monomers. Even for such a basic assumption interesting effects are obtained, as discussed here. To see this, we make use of the mean field parameter P_{AB} designating the probability that A and B are nearest neighbours. The value of this adjacency probability varies from $P_{AB} = 1/(M-1) \simeq 0$ in a block copolymer $(A)_{M/2}(B)_{M/2}$ to $P_{AB} = 1$ in a completely adjacent sequence, $(AB)_{M/2}$.[22,28] We study polymers with two different sequence patterns: one, for which the central part of the chain consists of A (B) monomers, around which the concentration of B (A) monomers is gradually increased. To be able to grasp this variation of monomer type, we consider three different regions of the chain, namely, domains with only A or B monomers, as well as domains built of AB blocks. The associated translocation velocities in our continuum approach are then given by

$$\begin{aligned} V_{AA} &= \frac{\sigma}{2\tau_0} P_{AA}, \\ V_{AB} &= \frac{\sigma}{2\tau_0} P_{AB}, \\ V_{BB} &= \frac{\sigma}{2\tau_0} P_{BB}. \end{aligned} \tag{21}$$

In the above sense, these three types of regions allow us to construct the chain-to-be-translocated symmetrically, with five regions, for instance,

$$BBBB\ldots ABAB\ldots AAAA\ldots BABA\ldots BBBB. \tag{22}$$

Altogether we thus have six boundaries, including the reflective and absorbing boundaries at the chain's extremities at $m = 0$ and $m = M$, respectively. For the intrachain boundaries, the total probability flux $j(x,t) = V\mathcal{P}(x,t) - D(\partial\mathcal{P}(x,t))/(\partial x)$ as well as the probability itself must be continuous (for more details, see Appendix B). Using the method introduced in Ref. 34 with these boundary conditions, we calculate the flux $j(L, s)$ of chain-exits at the pore to the trans side in Laplace space. We then invert this result numerically to the time domain, and thus reconstruct the overall PDF of polymer translocation times. In Fig. 6 we compare these results with simulations, observing good agreement, with no adjustable parameter. As expected, an exponential decay is observed.[38] Above findings provide additional insight into the translocation dynamics of heteropolymer chains, compared to previous studies of the translocation time dependence on chain-pore interactions of A_nC_n block copolymers in Ref. 39.

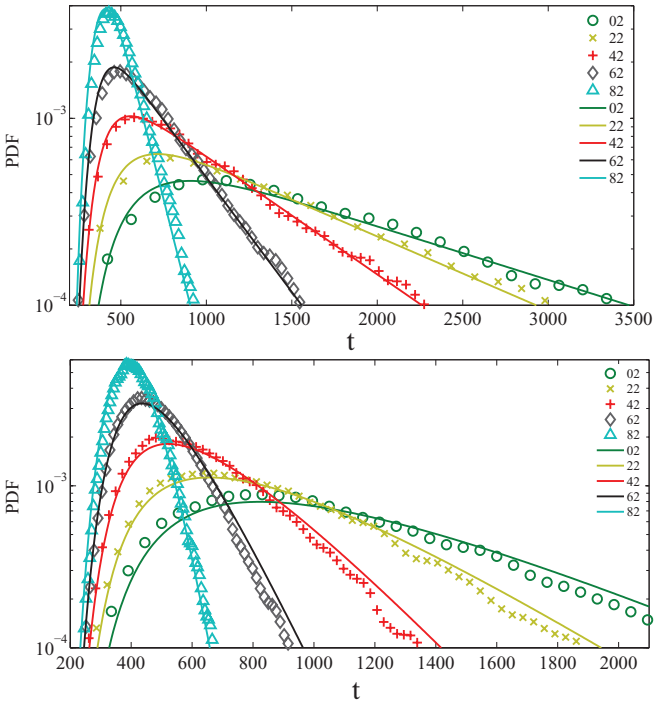

FIG. 6. Comparison of the transloaction time PDFs for polymers with effective binding energies $\mathcal{E}_{\rm eff}(A) = 2$ and $\mathcal{E}_{\rm eff}(B) = -2$ and with varying adjacency probabilities P_{AB} (indicated in % for the different curves in the plots). The PDFs are obtained from our theoretical model (Eq. (11)) by numerical Laplace inversion (full lines). These are compared to simulations (symbols). Left: Translocation time PDF for chains with central B monomers. Right: Translocation time PDF for chains with central A monomers. In the right graph both the maxima are shifted to longer times and the exponential tails are wider. Simulations points from Ref. 22.

IV. SAWTOOTH BEHAVIOR OF TRANSLOCATION DYNAMICS FOR $\lambda > 6$

In Sec. III we only considered chaperones that cover exactly $\lambda = 2$ chain monomers. To assess how different values of the chaperone size $\lambda\sigma$ affect the translocation time, we perform simulations for λ values between 2 and 10. In Fig. 7 we show the probability distribution $P(m, t)$ as function of the

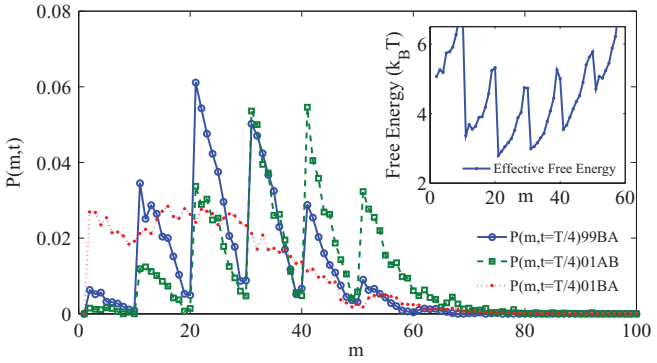

FIG. 7. Probability distribution $P(m, t)$ of the translocation progress, to find the chain with m translocated monomers at time $t \simeq T/4$, where T is the mean translocation time. The numbers before A, B indicate the value of P_{AB} in percent. We use the effective binding energies $\mathcal{E}_{\text{eff}}(A) = 2$ and $\mathcal{E}_{\text{eff}}(B) = -2$. The inset shows the negative of the logarithm of $P(m, t)$, that is a measure for the free energy at $t \simeq T/4$ as function of m in terms of k_BT, for a completely adjacent polymer ($P_{AB} \simeq 99\%$).

reaction coordinate at $t \simeq T/4$ for three polymer sequences with $\lambda = 10$. Note that for larger λ because of the summation over λ binding energies the transition between drift and diffusion dominated regimes will become increasingly sharp. At the same time a "parking-lot" effect is observed: after binding of a chaperone to the chain-to-be-translocated close to the membrane pore, the chain first needs to diffuse at least by the distance λ, before the next chaperone can bind next to the pore. This causes the sawtooth-shape in Fig. 7. For parts of the polymer chain consisting of monomers with negative EBE, the binding probability is near unity: as soon as a chaperone finds enough empty space, it will bind to the chain, and thus we see a ratchet-like PDF in this case. The inset in Fig. 7 also shows $-\ln(P(m, t))$, that is the effective free energy, as function of the reaction coordinate m at time $t \simeq T/4$, for a completely adjacent polymer.

Figs. 8 and 9 show the mean waiting time (MWT) and cumulative waiting time (CWT) for $\lambda = 6$. In analogy to the observations for the probability distribution in Fig. 7, we see a periodicity with length λ in the plot. This sawtooth behavior occurs for that polymer part, in which the EBE is negative, and it appears stronger when that part goes first.

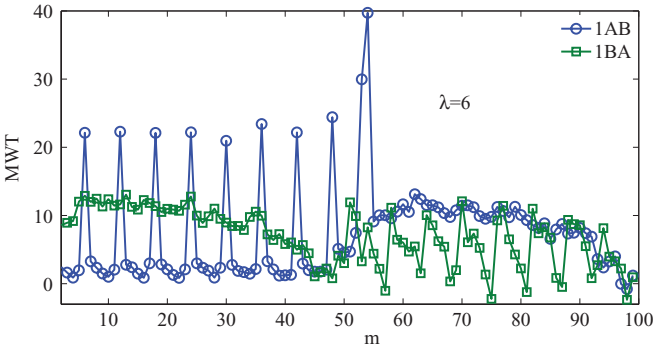

FIG. 8. It compares mean waiting times (MWTs) for $\lambda = 6$ and $E(A) = 0$, $E(B) = -2$ for a copolymer that goes through the pore from its two sides.

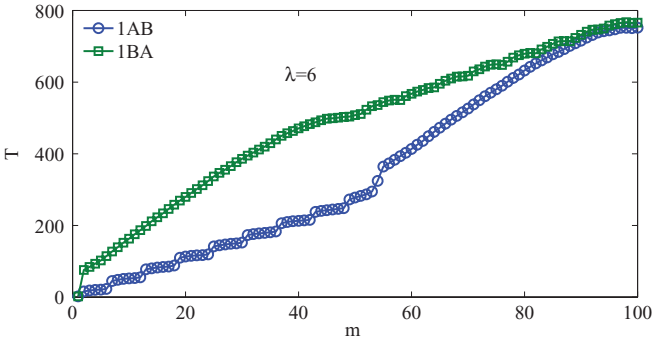

FIG. 9. It compares cumulative waiting times (CWTs) for $\lambda = 6$ and $E(A) = 0$, $E(B) = -2$ for a copolymer that goes through the pore from its two sides.

V. CONCLUSIONS

Based on a continuous drift-diffusion model, we obtain the full probability density function of passage times for chaperone-driven translocation of a stiff polymer. We consider both homopolymeric and heteropolymeric chains with different sequences. Comparison to Monte Carlo simulations shows very good overall agreement, such that for sufficiently long chains and large chaperone binding energy the drift-diffusion model is a good approximation to the full problem. Using this theoretical model we obtain the exponent α of the scaling relation $T \sim M^{\alpha}$ between mean translocation time T and number of monomers M of the chain-to-be-translocated. We also show how α is affected by the chain length, the binding energy and the chaperone concentration in solution. In particular we demonstrated that all relevant quantities, including the distribution of translocation times, is fully specified by the dimensionless Péclet number. We moreover discuss the effect of larger chaperone size on the probability distribution and mean waiting times of the translocation process, giving rise to pronounced sawtooth effects.

ACKNOWLEDGMENTS

We acknowledge financial support from the CompInt graduate school at TUM, from the Academy of Finland (FiDiPro scheme), as well as from Sharif University of Technology.

APPENDIX A: THE CONTINUUM TRANSITION

For long chains ($M\sigma \gg 1$) the size σ of an individual monomer becomes small, and we may therefore expand the master equation (4) as follows. To this end we change the notation from $P(m + 1, t)$ to $\mathcal{P}(x + \sigma, t)$, and from $W^{\pm}(m + 1)$ to $\mathcal{W}^{\pm}(x + \sigma)$, etc. As a result the corresponding continuum equation becomes

$$\frac{\partial \mathcal{P}(x,t)}{\partial t} = \frac{1}{2}\frac{\partial^2}{\partial x^2}[\sigma^2(\mathcal{W}^{+}(x) + \mathcal{W}^{-}(x))\mathcal{P}(x,t)] - \frac{\partial}{\partial x}[\sigma(\mathcal{W}^{+}(x) - \mathcal{W}^{-}(x))\mathcal{P}(x,t)]. \quad \text{(A1)}$$

Defining

$$D \equiv \frac{\sigma^2}{2}[\mathcal{W}^+(x) + \mathcal{W}^-(x)] = \frac{\sigma^2}{2\tau_0} \tag{A2}$$

and

$$V \equiv \sigma[\mathcal{W}^+(x) - \mathcal{W}^-(x)] = \frac{\sigma}{2\tau_0} P, \tag{A3}$$

we arrive at the advection-convection equation (9).

APPENDIX B: SOLUTION OF THE DRIFT-DIFFUSION EQUATION FOR A MAX-MIN SEQUENCE

Here we suppose that $\mathcal{E}_{\text{eff}}(A) = 2$ and $\mathcal{E}_{\text{eff}}(B) = -2$. For these EBE's the maximum sequences are defined as $(B)_{N_{BB}/2}(BA)_{N_{AB}/4}(A)_{N_{AA}}(AB)_{N_{AB}/4}(B)_{N_{BB}/2}$, in which $N_{AB} = P_{AB}(M-1)$, $N_{AA} = N_{BB} = ((M-1) - N_{AB})/2 = (M-1)(1-P_{AB})/2$. The minimum case is constructed in the same manner simply by exchanging A and B. We here find the first passage PDF for these types of polymers.

To solve Eq. (9), we pass to the Laplace space, in which we find

$$s\mathcal{P}(x,s) - \delta(x) + V\frac{\partial \mathcal{P}(x,s)}{\partial x} = D\frac{\partial^2 \mathcal{P}(s,t)}{\partial x^2}, \tag{B1}$$

in which we included the initial condition $P(x,0) = \delta(x)$. The result of this equation for a region with velocity V_i is then

$$\mathcal{P}_i(x,s) = A_+(i)e^{B_+(i)x} + A_-(i)e^{B_-(i)x}, \tag{B2}$$

where

$$B_\pm(i) = \frac{V_i \pm \sqrt{V_i^2 + 4Ds}}{2D} \equiv \text{Pe} \pm P_s, \tag{B3}$$

in which Pe is the Péclet number and P_s is defined in Eq. (13), and the $A_\pm(i)$ are obtained from the boundary conditions:

$$\left(V_1\mathcal{P}_1(x,s) - D_1\frac{\partial \mathcal{P}_1(x,s)}{\partial x} = 1\right)|_{x=0}, \tag{B4}$$

$$(\mathcal{P}_i(x,s) = \mathcal{P}_{i+1}(x,s))\,|_{x=L_i}(i = 1,4), \tag{B5}$$

$$\left(\frac{\partial \mathcal{P}_i(x,s)}{\partial x} = \frac{\partial \mathcal{P}_{i+1}(x,s)}{\partial x}\right)|_{x=L_i}(i = 1,4), \tag{B6}$$

$$(\mathcal{P}_5(x,s) = 0)\,|_{x=L}, \tag{B7}$$

in which L_is are defined for the maximum sequence as:

$$\begin{aligned} L_1 &= \sigma\left(\frac{N_{BB}}{2}\right), \\ L_2 &= \sigma\left(\frac{N_{BB}+N_{AB}}{2}\right), \\ L_3 &= \sigma\left(\frac{N_{BB}+N_{AB}}{2} + N_{AA}\right), \\ L_4 &= \sigma\left(\frac{N_{BB}}{2} + N_{AB} + N_{AA}\right), \end{aligned} \tag{B8}$$

and accordingly for the minimum sequence. For polymers with sequences introduced in Sec. III, there exist 5 regions, thus $i = 1,\ldots,5$ and we have 10 unknowns $A_\pm$. The boundary conditions provide 10 equations from which we obtain the 10 unknowns. From the boundary conditions at start and end of the translocation, we have respectively $j(0,s) = 1$ and $j(L,s) = 0$ [Eqs. (B4) and (B7)]. The remaining 8 equations are obtained from continuity of probability and flux at the four middle boundaries [Eqs. (B5) and (B6)]. Solving these equations provide the $A_\pm(i)$ and thus the probability in the Laplace space. We then numerically Laplace-invert this result. The theoretical results plotted in Fig. 6 are obtained in this way.

APPENDIX C: SIMULATIONS DETAILS

We use a Monte Carlo method to simulate the translocation process of polymers of size 100 monomers. Translocation of each of these polymers was performed 10^5 times. For each move of the polymer we bind and unbind the chaperones with Boltzmann probability for $5m$ times in which m is the number of monomers in the trans side, this number is selected to ensure equilibration.[22,30] To find the entire PDF of the translocation time numerically, we used the Metropolis approach. In the simulations, we attempt to move the polymer to the right and to the left with equal *a priori* probability. However, although the polymer may always move to the right, a move to the left is permitted only when the monomer next to the pore on the trans side is vacant. As in the theory, the boundary conditions in our simulations are reflecting at the left end and absorbing at the right end.

[1] B. Alberts, A. Johnson, J. Lewis, M. Raff, K. Roberts, and P. Walter, *Molecular Biology of the Cell* (Garland Publishing, New York, 2002).
[2] M. Akeson, D. Branton, J. J. Kasianowicz, E. Brandin, and D. W. Deamer, Biophys. J. **77**, 3227 (1999).
[3] M. Muthukumar, Annu. Rev. Biophys. Biomol. Struct. **36**, 435 (2007).
[4] T. A. Rapoport, Nature (London) **450**, 663 (2007).
[5] M. Muthukumar, J. Chem. Phys. **111**, 10371 (1999); Phys. Rev. Lett. **86**, 3188 (2001); J. Chem. Phys. **118**, 5174 (2003).
[6] K. Luo, R. Metzler, T. Ala-Nissila, and S.-C. Yung, Phys. Rev. E **80**, 021907 (2009).
[7] P. K. Purohit, M. M. Inamdar, P. D. Grayson, T. M. Squires, J. Kondev, and R. Phillips, Biophys. J. **88**, 851 (2005); *ibid.* **93**, 705 (2007).
[8] A. Meller, J. Phys. Condens. Matter **15**, R581 (2003).
[9] M. Wanunu, J. Suntin, B. McNally, A. Chow, and A. Meller, Biophys. J. **95**, 1193 (2008); A. J. Storm, C. Storm, J. H. Chen, H. Zandbergen, J. F. Joanny, and C. Dekker, Nano Lett. **5**, 1193 (2005); U. F. Keyser, B. N. Koeleman, S. van Dorp, D. Krapf, R. M. M. Smeets, S. G. Lemay, N. H. Dekker, and C. Dekker, Nat. Phys. **2**, 473 (2006); C. Dekker, Nat. Nanotechnol. **2**, 209 (2007).
[10] J. Li, D. Stein, C. McMullan, D. Branton, M. J. Aziz, and J. A. Golovchenko, Nature (London) **412**, 166 (2001); A. J. Storm, J. H. Chen, X. S. Ling, H. W. Zandbergen, and C. Dekker, Nature Mater. **2**, 537 (2003).
[11] J. J. Kasianowicz, E. Brandin, D. Branton, and D. W. Deamer, Proc. Natl. Acad. Sci. U.S.A. **93**, 13770 (1996).
[12] Y. Kantor and M. Kardar, Phys. Rev. E **69**, 021806 (2004).
[13] S. Matysiak, A. Montesi, M. Pasquali, A. B. Kolomeisky, and C. Clementi, Phys. Rev. Lett. **96**, 118103 (2006).
[14] K. Luo, T. Ala-Nissilä, S.-Ch. Ying, and R. Metzler, Europhys. Lett. **88**, 68006 (2009).
[15] J. Chuang, Y. Kantor, and M. Kardar, Phys. Rev. E **65**, 011802 (2001).
[16] D. K. Lubensky and D. R. Nelson, Biophys. J. **77**, 1824 (1999).
[17] J. O. Tegenfeldt, C. Prinz, H. Cao, R. L. Huang, R. H. Austin, S. Y. Chou, E. C. Cox, and J. C. Sturm, Anal. Bioanal. Chem. **378**, 1678 (2004).
[18] K. Luo and R. Metzler, J. Chem. Phys. **134**, 135102 (2011).
[19] W. Liebermeister, T. A. Rapoport, and R. Heinrich, J. Mol. Biol. **305**, 643 (2001).

[20]D. Tomkiewicz, N. Nouwen, and A. J. M. Driessen, FEBS Lett. **581**, 2820 (2007).
[21]J.-F. Chauwin, G. Oster, and S. Glick, Biophys. J. **74**, 1732 (1998).
[22]R. H. Abdolvahab, M. R. Ejtehadi, and R. Metzler, Phys. Rev. E **83**, 011902 (2011).
[23]S. F. Simon, C. S. Peskin, and G. F. Oster, Proc. Natl. Acad. Sci. U.S.A. **89**, 3770 (1992).
[24]W. Sung and P. J. Park, Phys. Rev. Lett. **77**, 783 (1996).
[25]R. A. Stuart, D. M. Cyr, E. A. Craig, and W. Neupert, Trends Biochem. Sci. **19**(2), 87 (1994).
[26]P. L. Krapivsky and K. Mallick, J. Stat. Mech.: Theory Exp. **2010**, P07007 (2010).
[27]R. Zandi, D. Reguera, J. Rudnick, and W. M. Gelbart, Proc. Natl. Acad. Sci. U.S.A. **100**, 8649 (2003).
[28]R. H. Abdolvahab, F. Roshani, A. Nourmohammad, M. Sahimi, and M. R. R. Tabar, J. Chem. Phys. **129**, 5102 (2008).
[29]T. Ambjörnsson, M. A. Lomholt, and R. Metzler, J. Phys. Condens. Matter **17**, S3945 (2005).
[30]T. Ambjörnsson and R. Metzler, Phys. Biol. **1**, 77 (2004).
[31]Y. Kafri, D. K. Lubensky, and D. R. Nelson, Biophys. J. **86**, 3373 (2004).
[32]T. Ambjörnsson and R. Metzler, J. Phys. Condens. Matter **17**, S1841 (2005).
[33]Wancheng Yu and Kaifu Luo, J. Am. Chem. Soc. **133**, 13565 (2011).
[34]S. Redner, *A Guide to First-Passage Processes* (Cambridge University Press, Cambridge, UK, 2001).
[35]See, for example, Ref. 21 and the disscusion in Ref. 22.
[36]C. W. Gardiner, Handbook of Stochastic Methods (Springer, New York, 2002).
[37]Note that $\langle V \rangle$ here is defferent fom V in Eq. (7). The $\langle V \rangle$ here is the mean first passage velocity, but the V in Eq. (7) is the average velocity without considering the boundary conditions (see for instance Ref. 36).
[38]C. Chatelain, Y. Kantor, and M. Kardar, Phys. Rev. E **78**, 021129 (2008).
[39]K. Luo, T. Ala-Nissila, S.-C. Ying, and A. Bhattacharya, Phys. Rev. Lett. **100**, 058101 (2008); J. Chem. Phys. **126**, 145101 (2007).